Photonic Crystal DFB laser array and fine emission wavelength engineering

O. Bouchard[1], A. Larrue[1], A. Monmayrant[1], O. Gauthier-Lafaye[1], S. Bonnefont[1],
P. Arguel[1] and F. Lozes-Dupuy[1],
C. Pang[2], A. Bruyant[2] and S. Blaize[2], G. Lérondel[2], P. Royer[2]
F. Pommereau[3], F. Poingt[3], L. Le Gouezigou[3], O. Le Gouezigou[3], O. Drisse[3], E. Dérouin[3]
and G. H. Duan[3]

[1]LAAS-CNRS Université de Toulouse, 7 avenue du colonel Roche, 31077 Toulouse Cedex 4, France
antoine.monmayrant@laas.fr
[2]LNIO, ICD CNRS (FRE2848), Université de Technologie de Troyes, 12, rue Marie Curie, BP2060.10010, Troyes cedex, France

[3]Alcatel Thales III-V Lab, Route départementale 128 -91767 Palaiseau Cedex, France

Abstract. *We report on Photonic Crystal DFB laser array under electrical pumping. The 2D geometry of the Photonic Crystal allows precise and fine wavelength spacing. Lasing occurs on the first excited mode, which can be explained by 2D-FDTD calculation showing extremely low loss and high DFB coupling for this mode.*

Introduction

All photonic crystal (PhC) defect waveguide lasers appear as extremely promising for planar optical integration. Indeed they are by nature fully compatible with already reported integrated compact optical systems based on PhC. Moreover, previous works have shown that such lasers can exhibit single-mode DFB-like operation [1] and have also predicted that precise wavelength engineering could be achieved by harnessing the transverse dimension of the 2D PhC [2].

Here we report on integrated arrays of defect waveguide lasers “SW5” where the wavelength spacing is set by altering the transverse period of each waveguide PhC. Both single- and dual-mode DFB lasers were obtained and using planar simulations we can explain most of these lasers' properties.

Sample and geometry

We focused on “SW5” defect waveguides obtained by omitting 5 rows of holes in a rectangular PhC, as shown on figure 1. Such lattice can be described by two periods: a , along the waveguide, and b, transverse to the waveguide. The former is set to a=484 nm for all the lasers in the array and we vary the latter to change the wavelength. In practice, both lattice constants differ by only few percents and we stay close to a square geometry (a~b). Each waveguide can be seen as a square lattice that has been laterally shrinked or expanded by an affine deformation while keeping the hole radius constant. The dimensionless **deformation**, that we define as $\alpha=b/a$, is the key design parameter in this work and all the other parameters remain constant.

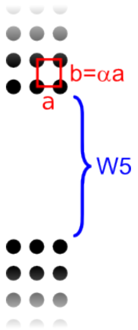

Figure 1: SW5 photonic crystal defect waveguide.

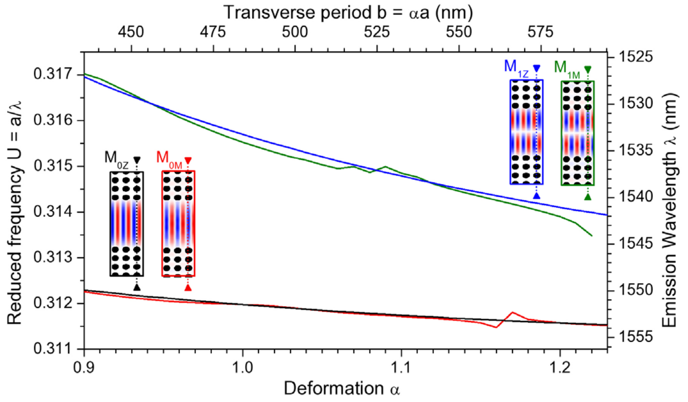

Figure 2:2D-FDTD simulations: wavelength of the first 4 DFB modes: fundamental M_{0Z} (black) and M_{0M} (red) and 1st excited M_{1Z} (blue) and M_{1M}(green). Insets show each mode inside the guide.

For this study, we built arrays of 12 lasers, with a period a=484 nm, hole radius of r=150 nm and deformations ranging from α=0.91 to α=1.23. The waveguides were 370 µm long and both ends were 15 µm away from the cleaved edge. These 15 µm of free propagation help reducing the re-injection from the cleaved edge and ensure a reproducible DFB operation.

Samples were fabricated at "Alcatel Thales III-V Lab" in the InGaAsP/InP material system. We used an InGaAsP planar waveguide on InP substrate with 6 compressively quantum wells. The gain curve of the quantum wells is centered around 1550 nm. The PhC waveguides were defined using e-beam lithography and deep dry etching. The holes depth is around 4 µm, deep enough to achieve 2D like geometry. Metallic contacts were then deposited on the top and bottom surfaces, taking care not to fill the holes so as to preserve the quality of the PhC. A gain region of around 10 µm wide was delimited by proton implantation. Samples were then thinned and cleaved into laser arrays that we reported on an aluminum submount, in turn mounted on a PCB board for characterization.

These structures were simulated using 2D FDTD [3], with an effective index of n_{eff}=3.21 and assuming an infinitely long waveguide (periodic boundaries). The effect of the lateral implant on the guided mode was described using weak perfectly matched layers (PML) in the implanted regions.

Figure 2 shows the evolution of the emission wavelength with the deformation for 4 first DFB modes. The two degenerated fundamental modes are M_{0Z} (black) and M_{0M}(red) and the two degenerated first excited modes are M_{1Z} (blue) and M_{1M}(green). The subscripts "Z" and "M" respectively stand for "zero" and "maximum" and describe the way the mode is phased with the holes, as can be seen on the insets of figure 2: "Z" modes have a zero aligned with the holes column and "M" modes have a maximum aligned with the holes column. "M" modes experience higher losses than "Z" ones and this explains the single-mode operation on the M_{0Z} reported for W1 waveguides [1].

Here, we expected single-mode DFB operation on M_{0Z}, with a central wavelength ranging from 1550 nm to 1554 nm, as can be seen on figure 2 (black line).

Experimental results

Emission spectra of the lasers were measured under pulsed operation using a 1-m focal length monochromator fitted with a cooled InGaAs photomultiplier. Figure 3 shows the DFB lasing wavelength depending on the deformation α (top part) together with a typical spectrum obtained for deformation α=1 (bottom part).

As expected, the lasing wavelength changes slowly and linearly with the deformation.

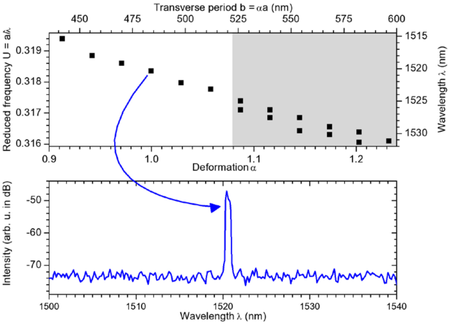

Figure 3:Lasing wavelength depending on the deformation (top) and typical spectrum (bottom). In the gray area (top) lasers are dual-mode.

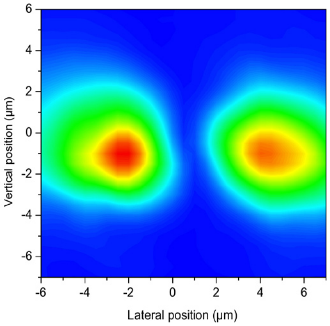

Figure 4: Beam profile measured in the close vicinity of the cleaved edge on a SW5 waveguide for α=1.

However, neither the average lasing wavelength (around 1520 nm) nor the slope of the wavelength evolution ($\Delta\lambda/\Delta b\approx0.1$) matches what was expected for the fundamentals DFB modes M_{0Z} and M_{0M} (see figure 2). In fact, all these lasers are on the first excited transverse mode. Indeed, the theoretical slope for M_{1Z} and M_{1M} ($\Delta\lambda/\Delta b\approx0.1$) perfectly matches the experimental results shown on figure 3 (we attribute the small wavelength offset to a slight mismatch in the effective index used in the simulation).

Lasing on the first excited mode was confirmed by near-field probe measurements in the close vicinity of the waveguide exit facet. To avoid distortion of the beam profile over the 15 µm of free propagation, measurements were made on shorter lasers (280 µm long) cleaved inside the waveguide. Figure 4 shows a typical intensity profile obtained for a cleaved SW5 waveguide for α=1 (lasing wavelength around 1520 nm).

Moreover, for deformations higher than α=1.08 (gray area), the lasers are no longer single-mode and both degenerated DFB modes M_{1Z} and M_{1M} are visible.

Analysis and discussion

To understand why these lasers were on the first excited mode and why the single-mode behavior was lost for high deformations, we compared various properties of the different modes obtained from 2D FDTD and complementary 2D plane wave simulations.

First, from the spatial profile of each mode, we estimated the confinement inside the guide and thus the modal gain. We found that all 4 modes experience almost identical modal gain (with a confinement above 98 %).

Then, we extracted from 2D-FDTD the loss level (the imaginary part of the propagation constant) for each mode, which is displayed on figure 5. One of the first excited mode, M_{1Z} (blue), experiences losses orders of magnitude smaller then the other 3 modes excepted for high deformations where the loss level difference tend to shrink.

This low level of losses for M_{1Z} , together with comparable modal gain could explain the single-mode lasing on the first excited mode observed in our experiment.

Moreover, there is a clear reduction in the loss level difference for high deformations, in good agreement with the experimental observation of a dual-mode behavior for the DFB lasers. This reduction could partly explain the dual mode behavior seen experimentally.
However, for high deformations, fundamental modes M_{0Z} (black) and M_{0M} (red) also experience reduced losses, whereas we never see lasing on of these modes. An explanation could lay in the DFB coupling that is way stronger for the first excited modes than the fundamental ones in this region.
Once more, these 2D simulations only account for in-plane losses and 3D FDTD simulations are needed to estimate losses out of the plane that could be different for fundamental and first order modes.

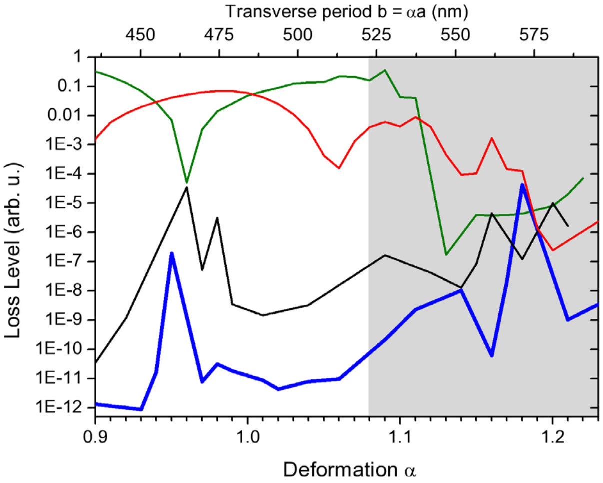

Figure 5:Loss level for the first 4 DFB modes, M_{0Z} (black), M_{0M}(red), M_{1Z} (blue) and M_{1M}(green). M_{1Z} (blue) has lower losses than all the other modes. The gray area corresponds to deformations for which lasers are dual-mode.

Conclusion

We have experimentally demonstrated a new concept for integrated DFB laser arrays based on PhC defect waveguide. The affine deformation of the crystal lattice offers an efficient way to precisely tailor the wavelength spacing between lasers of the array. The peculiar characteristic of these lasers, among which the lasing on the first excited transverse mode, is well described by planar simulations.

A. Larrue acknowledges financial support from DGA under supervision of B. Desruelle.

References

[1] Gauthier-Lafaye O et al.. "Highly monomode w1 waveguide square lattice photonic crystal lasers." *IEEE Photonics Technology Letters* (2005) **17**: pp. 1587-1589.
[2] Gauthier-Lafaye O et al.. Square lattice w1 waveguide photonic crystals lasers for telecommunications. In *Proceedings of spie "photonic materials, devices, and applications"*. 2005.
[3] Farjadpour A et al.. "Improving accuracy by subpixel smoothing in the finite-difference time domain." *Opt. Lett.* (2006) **31**: p. 2972--2974.